DOI: 10.1002/cjoc.201600885

Detection of Picric Acid by Terpy-Based Metallo-Supramolecular Fluorescent Coordination Polymers in Aqueous Media

Zhongyu Ding,[a] Hongqing Li,[a] Wanqing Gao,[a] Yiquan Zhang,[b] Chunhua Liu,*[,a] and Yuanyuan Zhu*[,a]

[a] *School of Chemistry and Chemical Engineering*, *Hefei University of Technology and Anhui Key Laboratory of Advanced Functional Materials and Devices*, *Hefei*, *Anhui 230009*, *China*
[b] *Jiangsu Provincial Key Laboratory for Numerical Simulation of Large Scale Complex Systems* (*NSLSCS*), *School of Physical Science and Technology*, *Nanjing Normal University*, *Nanjing*, *Jiangsu 210023*, *China*

The synthesis of two linear terpy-based metallo-supramolecular fluorescent coordination polymers through 1∶1 complexation of Zn^{2+} and Cd^{2+} ions with ditopic terpyridine ligand was reported. The dispersibility of **P1** and **P2** was significantly improved in organic solvent and water through the introduction of hydrophilic oligo-ethyoxy side chain. Two polymers displayed yellow light emission both in solution and the solid state due to the intra-ligand charge transfer (ILCT) between the d^{10} metal ions and the conjugated spacer unit. These coordination polymers were explored as fluorescent chemosensors for detecting picric acid in aqueous media, displaying high sensitivity and good selectivity. In addition, test strips were prepared from these polymers and exhibited the practical potential of detecting the NACs pollutants in the outdoor water for public safety and security.

Keywords coordination polymer, fluorescent chemosensors, nitroaromatic explosives, picric acid, aqueous media

Introduction

Fluorescence is a simple but powerful signal transduction method for the formation of chemosensory devices.[1] Recently, the development of new efficient fluorescence quenching "turn-off" methods for the detection of nitroaromatic explosives (NACs), especially for picric acid (PA), has received great research interest.[2] Besides, as a powerful explosives,[3] PA is also widely used in dye and pharmaceutical industries and in chemical laboratories.[4] Because of its excellent solubility in water, it can easily contaminate outdoor water and groundwater when exposed. Medical research demonstrated that intake of PA may cause skin and eye irritation and other chronic diseases.[5] Hence, for preventing terrorist threats and environmental pollution, development of efficient sensors to detect PA and other NACs at very low concentrations is a very appealing and urgent research area in scientific society.[6]

Currently, various methods have been established for the detection of NACs. Among them, fluorescence sensing is widely investigated because of its advantages of high sensitivity, quick response, low cost efficiency, easy sample preparation, *etc*.[7] Up to date, several π-electron-rich fluorescent organic polymers,[8] coordination polymers (CPs)/metal-organic frameworks (MOFs),[9] supramolecular polymers,[10] organic molecules,[11] and nanostructures[12] have been employed to detect the presence of electron-deficient nitroaromatics. However, most detection methods were performed in organic solution. Therefore, the development of suitable soluble and efficient organic fluorescent chemosensors (FCs) with high sensitivity and selectivity for PA in aqueous media is still a very challenging task.

Metallo-supramolecular coordination polymers belong to a new type of organic/inorganic hybrid material that combines the common features of traditional covalently bound polymers with the properties imposed by coordination metal ions.[13] Among them, d^{10} transition metals (such as Zn^{2+} and Cd^{2+}) based coordination polymers can display excellent photoluminescent (PL) electroluminescent (EL) properties. In these coordination polymers, the intra-ligand charge transfer (ILCT) between the d^{10} coordination site and the chromophore of the ligand generates strong luminescence and the wavelength and intensity of emission can be fine tuned through the structural design of ligands. Several examples demonstrated that the mediation of emission color

* E-mail: yyzhu@hfut.edu.cn, lchh88@hfut.edu.cn
Received December 13, 2016; accepted February 22, 2017; published online April 10, 2017.
Supporting information for this article is available on the WWW under http://dx.doi.org/10.1002/cjoc.201600885 or from the author.
Dedicated to Professor Xi-Kui Jiang on the occasion of his 90th birthday.

and enhanced luminescence could be achieved through rational ligand design.[14]

The luminescence of coordination polymers will undergo "turn-off" changes caused by electron or energy transfer from excited-state of electron-rich fluorophores to ground-state of electron-deficient nitrated organic compounds.[15] So we proposed to use soluble luminescent coordination polymers serving as FCs for detection of trace NACs. In previous work, we synthesized a series of Zn(II) metallo-supramolecular coordination polymers based on tridentate pyridine-2,6-bis-(oxazoline) ligands and demonstrated the fluorescence tuning and the highly sensitive and selective detection of trace PA both in organic solution and the solid state. These types of polymers, however, are unstable in polar solvents including DMF, DMSO, and H_2O.[16] This disadvantage impedes the practical application of detection in aqueous media. In order to solve this problem, we propose using strong coordinated terpydine (terpy) to replace pybox to enhance the stability of polymers in polar solvents and introducing tetraethyleneglycol monomethyl ether side chain into the ligand to improve the solubility of polymers in aqueous media.[17,18] In this contribution, we report on the synthesis of two terpy based metallo-supramolecular fluorescent coordination polymers and the achievement of PA detection in aqueous media.

Experimental

Materials and equipments

Melting point was uncorrected. The NMR spectra were performed on a Bruker 400 MHz or 600 MHz spectrometer. The chemical shifts (δ) in ^{1}H NMR were reported relative to tetramethylsilane (Me_4Si) as internal standard (δ 0.0) or proton resonance resulting from incomplete deuteration of NMR solvent: $CDCl_3$ (δ 7.26) or DMSO-d_6 (δ 2.50). Coupling constants (J) are expressed in hertz. ^{13}C NMR spectra were recorded at 100 MHz or 125 MHz, and the chemical shifts (δ) were reported relative to $CDCl_3$ (δ 77.10) or DMSO-d_6 (δ 40.50). Mass spectra were recorded on a Bruker Solarix Fourier Transform Ion Cyclotron Resonance Mass Spectrometer. Elemental analysis of carbon, nitrogen and hydrogen was performed using an Elementary Vario EL analyzer. UV-vis spectra were recorded using a SHIMAD2U UV-2550 spectrometer. Emission spectra were recorded using a Hitachi F-4600 fluorescence spectrophotometer.

All solvents were purchased from Sinopharm and used without further purification unless otherwise denoted. Tetrahydrofuran, ethanol, and acetonitrile were further dried over calcium hydride, and distilled under high vacuum just before use. All chemicals were purchased from Aladdin, Aldrich, Alfa Aesar and Sinopharm, and were used as received.

Synthesis of 1[19]

To a suspension of 1,4-dihydroxybenzene (0.05 mol, 5.5 g) in glacial acetic acid (50 mL) under stirring, bromine (0.1 mol, 5.2 mL) in glacial acetic acid (5 mL) was carefully added dropwise. After the completion of adding, the solution was still stirred at ambient temperature for 6 h. Then the resulting solution was poured in water (100 mL) and extracted from ethyl acetate (50 mL×3). The combined organic layer was dried over anhydrous Na_2SO_4 and concentrated under reduced pressure. The resulting solid was washed with a little glacial acetic acid to give the product as a white solid (10.85 g, 81%). ^{1}H NMR (600 MHz, DMSO-d_6) δ: 9.84 (s, 2H), 7.04 (s, 2H).

Synthesis of 2[20]

10.4 g (50 mmol) of tetraethyleneglycol monomethyl ether was taken into THF (25 mL) and cooled in an water-ice bath. To the cooled solution, sodium hydroxide (6.0 g, 150 mmol) in water (25 mL) was added. *p*-Tosyl chloride (12.4 g, 65 mmol) in THF (15 mL) was then added slowly (over 30 min). Then the reaction solution was allowed to warm up to ambient temperature and stirred overnight. After completion of reaction, the separated organic layer was collected and the aqueous layer was extracted twice with diethyl ether (25 mL×2). The combined organic layer was washed with 10% sodium hydroxide solution, followed by water and saturated brine. Then the organic phase was dried over anhydrous Na_2SO_4, filtered and concentrated to obtain the pure product as colorless viscous liquid in nearly quantitative yield. ^{1}H NMR (400 MHz, $CDCl_3$) δ: 7.78 (d, J=8.0 Hz, 2H), 7.33 (d, J=8.0 Hz, 2H), 4.14 (t, J=4.8 Hz, 2H), 3.73 (t, J=6.4 Hz, 2H), 3.67 (t, J=4.8 Hz, 2H), 3.63−3.61 (m, 6H), 3.57 (s, 4H) , 3.54−3.52 (m, 2H), 3.36 (s, 3H), 2.43 (s, 3H).

Synthesis of 3[20]

The solution of **1** (0.94 g, 3.5 mmol) and K_2CO_3 (1.93 g, 14 mmol) in acetonitrile (40 mL) was heated under reflux in an N_2 atmosphere for 30 min. The solution of **2** (2.79 g, 7.7 mmol) in acetonitrile (4 mL) was added dropwise to the mixture, stirring and refluxing were continued for 24 h. The reaction mixture was then filtered and the solvent was removed *in vacuo*. The residue was purified by column chromatography (SiO_2/Ethyl acetate) to yield **3** as a yellow liquid (1.42 g, 63%). ^{1}H NMR (400 MHz, $CDCl_3$) δ: 7.14 (s, 2H), 4.12 (t, J=4.8 Hz, 4H), 3.87 (t, J=4.8 Hz, 4H), 3.76 (m, 4H), 3.69−3.63 (m, 16H), 3.55−3.53 (m, 4H), 3.37 (s, 6H).

Synthesis of 4[21]

4-Formylphenylboronic acid (3.36 g, 20 mmol), 2-acetylpyridine (5.32 g, 44 mmol), and powdered NaOH (4.80 g, 120 mmol) were added to absolute EtOH (150 mL) in a round bottom flask. After stirring at ambient temperature for 5 h until 4-formylphenylboronic acid was all consumed (monitored by TLC), the color of solution changed from yellow to red. Then a concentrated aqueous NH_3 solution (60 mL) was added and the

suspension was stirred at 65 ℃ for 12 h to give a dark yellow solution with a colorless precipitate. The precipitate was filtered under reduced pressure and washed with a little amount of isopropanol and chloroform to give product as a nearly colorless solid (4.6 g, 65%). ^{1}H NMR (400 MHz, CD_3OD) δ: 8.71－8.63 (m, 6H), 8.01 (td, J=7.6, 2.0 Hz, 2H), 7.75 (d, J=8.4 Hz, 2H), 7.73 (d, J=8.4 Hz, 2H), 7.47 (ddd, J=7.2, 4.8, 0.8 Hz, 2H).

Synthesis of L

A mixture of **3** (520 mg, 0.8 mmol), **4** (932 mg, 2.4 mmol), $Pd(PPh_3)_2Cl_2$ (59 mg, 0.08 mmol), K_2CO_3 (884 mg, 6.4 mmol), and mixed solvent [V(toluene)/V(t-BuOH)/V(H_2O), 9∶3∶9] was placed into a 100 mL sealed container with a magnetic stirring bar and evacuated and purged with nitrogen. Then the mixture was heated to 95 ℃ and refluxed for 2 d. After cooling to room temperature, the reactant was extracted with chloroform. The combined organic layers were dried over anhydrous Na_2SO_4. After the removal of solvent, the resulting yellowish solid was recrystallized from the mixture of methanol and chloroform to obtain the pure product as white solid (430 mg, 64%). M.p. 183－185 ℃. ^{1}H NMR (600 MHz, $CDCl_3$) δ: 8.82 (s, 4H), 8.76－8.75 (m, 4H), 8.70 (d, J=8.4 Hz, 4H), 8.00 (d, J=8.4 Hz, 4H), 7.90 (t d, J=7.8, 1.8 Hz, 4H), 7.80 (d, J=8.4 Hz, 4H), 7.37 (ddd, J=7.2, 4.8, 0.6 Hz, 4H), 7.12 (s, 2H), 4.16 (t, J=4.8 Hz, 4H), 3.80 (t, J=4.8 Hz, 4H), 3.67－3.65 (m, 4H), 3.63－3.62 (m, 8H), 3.61－3.59 (m, 4H), 3.57－3.56 (m, 4H), 3.47－3.46 (m, 4H), 3.31 (s, 6H); ^{13}C NMR (125 MHz, $CDCl_3$) δ: 156.28, 155.99, 150.59, 149.90, 149.14, 138.97, 137.05, 136.84, 130.72, 130.12, 126.93, 123.82, 121.36, 118.72, 116.82, 71.86, 70.82, 70.66, 70.59, 70.55, 70.43, 69.80, 69.54, 58.93. MS (XR-FT) m/z: 1105.5 $[M+1]^+$. Anal. calcd for $C_{66}H_{68}N_6O_{10}$: C 71.72, H 6.20, N 7.60; found C 71.34, H 5.98, N 7.99.

Synthesis of P1

An equimolar amount of the ditopic ligand **L** and $Zn(ClO_4)_2$ was stirred at 85 ℃ in the mixed solvent of acetonitrile and chloroform (V/V, 1∶1) under an N_2 atmosphere for 24 h (*ca*. 1 mL solvent per 2 mg of the ligand). After the reaction solution was cooled to ambient temperature, diethyl ether was added slowly to form the yellow precipitate. The precipitated polymers were collected by filtration under reduced pressure, washed with diethyl ether three times, and then dried *in vacuo* to give the corresponding metallo-supramolecular polymers as a yellow powdered solid with yield of 87%. ^{1}H NMR (600 MHz, $CDCl_3$) δ: 9.44－7.58 (m, 28H), 7.28 (s, 2H), 4.27 (s, 4H), 3.76 (s, 4H), 3.58－3.30 (m, 24H), 3.12 (s, 6H); ^{13}C NMR (100 MHz, $CDCl_3$) δ: 150.12, 149.60, 148.01, 147.86, 147.47, 141.45, 134.26, 130.46, 129.48, 128.03, 127.88, 123.62, 121.12, 120.36, 116.18, 71.27, 70.03, 69.97, 69.91, 69.85, 69.61, 69.22, 68.77, 58.05. Anal. calcd for $C_{68}H_{68}F_6N_6O_{16}S_2Zn$: C 55.61, H 4.67, N 5.72; found C 56.57, H 5.04, N 5.23.

Synthesis of P2

P2 was prepared from **L** and $Cd(ClO_4)_2$ as a yellow powdered solid in 91% yield according to a procedure similar to that for **P1**. ^{1}H NMR (600 MHz, $CDCl_3$) δ: 9.11－7.98 (m, 24H), 7.60 (br, 4H), 7.28 (s, 2H), 4.27 (s, 4H), 3.77 (s, 4H), 3.60－3.30 (m, 24H), 3.12 (s, 6H); ^{13}C NMR (100 MHz, $CDCl_3$) δ: 150.12, 149.60, 148.01, 147.86, 147.47, 141.45, 134.26, 130.46, 129.48, 128.03, 127.88, 123.62, 121.12, 120.36, 116.18, 71.27, 70.03, 69.97, 69.91, 69.85, 69.61, 69.22, 68.77, 58.05. Anal. calcd for $C_{68}H_{68}CdF_6N_6O_{16}S_2$: C 53.88, H 4.52, N 5.54; found C 54.79, H 5.33, N 4.91.

UV-vis titration in organic media

The UV-vis titrations of ligand **L** with Zn^{2+} and Cd^{2+} ions in organic solvents were carried out by placing 2 mL chloroform solution of ligand (4.0×10^{-5} mol•L^{-1}) in a quartz cuvette of 1 cm width. At 25 ℃, the dilute solution of $Zn(ClO_4)_2$ or $Cd(ClO_4)_2$ in methanol (1.0×10^{-3} mol•L^{-1}) was added in an incremental fashion. The absorption of additives was deducted through adding the solution of additives into the cuvettes of sample solution and background solvent simultaneously before measurement.

Photoluminescence measurements

For fluorescence measurements, ligand and polymers were excited at their λ_{max} of UV absorption and their emissions were monitored within the suitable region while keeping 5.0 nm slit width for both source and detector at 400 V voltage.

Fluorescence quenching titration with NACs in aqueous media

The fluorescence quenching titrations with different NACs in aqueous media were carried out by placing 2 mL aqueous solution of two polymers **P1** and **P2** in a quartz cuvette of 1 cm width. Then, the aqueous or methanol solution of several NACs was added in an incremental fashion at 25 ℃. Two polymers were excited at their λ_{max} of UV absorption and their emissions were monitored within the suitable region while keeping 10.0 nm slit width for both source and detector and voltage as 700 V.

The fluorescence quenching efficiency (η) for each of NACs was calculated by the following equation:

$$\eta=(I_0-I)/I_0\times100\%$$

where I_0 and I are the fluorescence intensities in the absence and presence of NACs, respectively.

Calculation of the Stern-Volmer constant

The sensitivity of two polymers toward PA was estimated from the Stern-Volmer constant (K_{SV}). The Stern-Volmer plots were plotted as a function of the PA concentration ([C]) in the following equation:

$$I_0/I-1=K_{SV}\times[C]$$

Thus, K_{SV} can be calculated from the slope of the linear Stern-Volmer plot obtained at low concentration range of PA.

Visual detection of PA on dip-coated test strips under UV light

A piece of filter paper (3.0 cm×1.0 cm) was immersed in a chloroform solution of **P1** and **P2** (1×10^{-4} mol•L^{-1}) for 5 min. Then, the filter paper was removed from the solution and dried under vacuum. Under illumination with a UV lamp at 365 nm, the filter paper emitted strong yellow fluorescence. To demonstrate its application as a fluorescence paper sensor for the detection of PA, the test strips were dipped into aqueous solution of PA at very low concentration (1.0×10^{-6} mol•L^{-1}), and no emission could be observed under 365 nm UV light. The images were obtained under UV illumination at 365 nm.

DFT calculation

Orca 3.0.3 calculations[22a] were performed with the popular hybrid functional B3LYP method to optimize these structures, and then obtain the dipole moments and also the energy gaps between HOMO and LUMO of the optimized structures. Triple-ζ with one polarization function TZVP[22b,22c] basis sets was used for all atoms, and zero order regular approximation (ZORA) was used for the scalar relativistic effect in all calculations.

Results and Discussion

Preparation of ditopic ligand and Zn(II)/Cd(II)-based metallo-supramolecular coordination polymers

Ligand **L** was synthesized via palladium-catalyzed Suzuki coupling reaction of bromined substrate **3** with boric acid linked terpy substrate **4** (Scheme 1). Subsequently, metallo-supramolecular polymers **P1** and **P2** were prepared by 1∶1 complexation of $Zn(ClO_4)_2$ or $Cd(ClO_4)_2$ with **L** under reflux in the mixed solvent of acetonitrile and chloroform (*V*/*V*, 1∶1) for 24 h (Scheme 2). The polymers were purified by repeated

Scheme 1 The synthetic route of ditopic ligand **L**

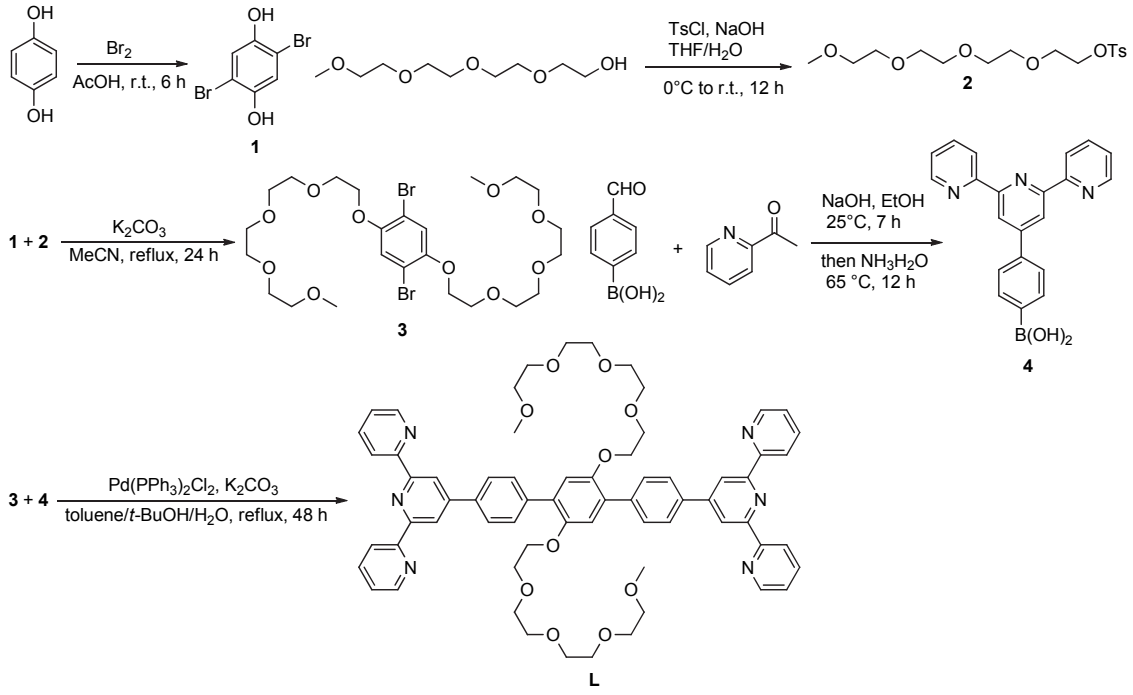

Scheme 2 The synthetic route of **P1** and **P2**

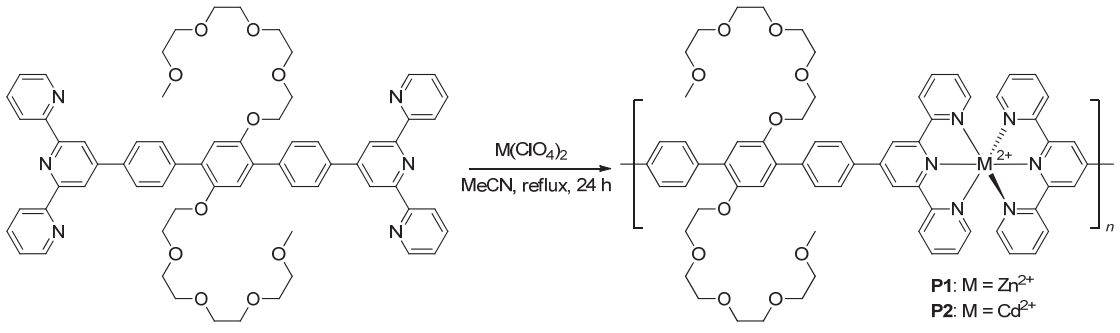

precipitations from acetonitrile in diethyl ether. Both polymers exhibited good stability and solubility in polar solvents such as DMF and DMSO. The polymers can not be dissolved directly in other less polar solvents due to their strong electrostatic interaction between the polyelectrolytes and counter anions. However, after dissolving in a little amount of DMF, the polymers can stably dispersed in solvents including dichloromethane, chloroform, acetone, acetonitrile, water, *etc*.

Absorption spectra

The investigations of absorption spectra for ligand and polymers were carried out in chloroform firstly. The absorption of **L** displays two maxima (λ_{max}) at 289 and 326 nm, corresponding to the π-π* transitions of the conjugated core. Compared with that of ligand, the absorptions of two polymers display a significant red-shift because of the inductive effect of the metal ions (Figure 1). In chloroform, **P1** and **P2** show the lowest energy absorbance maxima (λ_{max}) at 389 nm and 385 nm, respectively [Figure 1(a)]. The solvent effects on the absorption for the ligand and polymers were tested in detail. Overall, the polymers display blue-shift with increasing solvent polarity [Figures 1(b) and S13].

Homogenous thin films of **P1** and **P2** were prepared on a quartz glass substrate by dipping their chloroform solutions (Figure S14). Their films show a slight red-shift of lowest energy absorption maxima compared to those in low polar solution. It is consistent with our previous observation in pybox series coordination polymers,[16] which may originate from the enhanced intermolecular interaction between the polymer chains in the solid state.

The metal-ion-mediated self-assembly processes were investigated in depth by the variation of absorption spectra. We titrated the chloroform solution of **L** with $Zn(ClO_4)_2$ and $Cd(ClO_4)_2$ and monitored the processes through UV-vis spectroscopy (Figure 2). Our measurements demonstrated that the titration of **L** at a concentration of 4.0×10^{-5} mol/L with up to 1 equiv. of $Zn(ClO_4)_2$ caused a significant red-shift in the absorption spectra. The originally strong lowest-energy absorption of **L** at 287 nm was gradually red-shifted to 387 nm because of the intramolecular charge transfer from the electron rich central terphenyl component to the metal ion-coordinated, electron-deficient terpy moiety. Upon the addition of $Zn(ClO_4)_2$, the intensity of the absorption peak of ligand at 287 nm continuously decreased and the absorption peak of the polymer at 387 nm increased in a linear fashion, until a metal-to-ligand ratio of 1∶1 was attained, implying the association constant for the polymerization process. The appearance

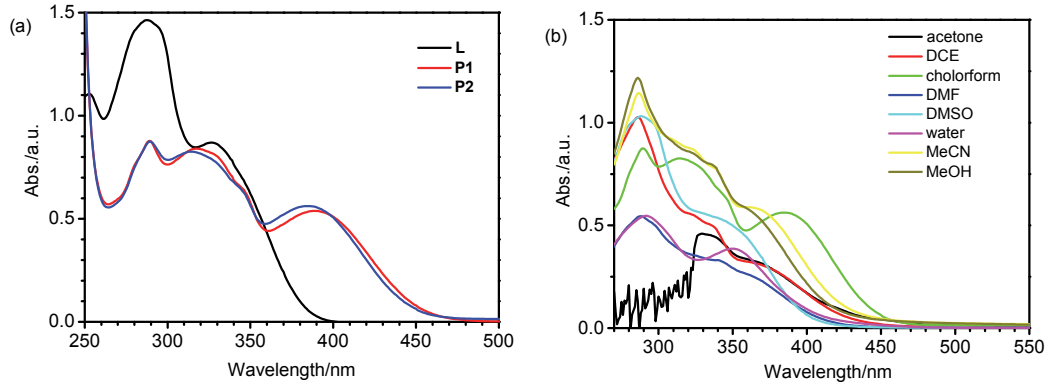

Figure 1 (a) UV-vis absorption spectra of **L**, **P1**, and **P2** in the chloroform solution (4.0×10^{-5} mol/L); (b) UV-vis absorption spectra of **P2** in different solvents (4.0×10^{-5} mol/L).

Table 1 UV-vis spectral data of **L**, **P1**, and **P2** in different solvents and polymer films

Solvent	Solution						Film	
	λ_{abs}[a]/nm			$\varepsilon\times10^4$[b]/(mol^{-1}•L•cm^{-1})			λ_{abs}[c]/nm	
	L	**P1**	**P2**	**L**	**P1**	**P2**	**P1**	**P2**
Acetone	332	329, 370	329	2.20, 1.15	1.74	1.15		
DCE	253, 288, 327	287, 324	286	2.85, 3.84, 2.23	7.71, 2.57, 1.90	2.57		
$CHCl_3$	253, 288, 326	322, 386	321, 387	2.76, 3.66, 2.18	2.86,1.71	2.41, 1.48		
DMF	288	287	288	3.66	2.26	1.36	287	290
DMSO	289	289	288	2.48	3.35	2.58	325 369	382
H_2O	293, 355	289	292, 350	0.16, 0.54	1.85	1.37, 0.97		
MeCN	251, 286, 327	286	287	2.59, 3.43, 1.84	3.33, 2.65, 1.73	2.86		
MeOH	249, 286	286	286	2.69, 3.76	2.70, 2.13, 1.34	3.04		

[a] 4.0×10^{-5} mol/L in different solvents; [b] Extinction coefficients at the lowest-energy absorption band. [c] Thin film on a quartz glass substrate.

of an isosbestic point at 305 nm suggested the equilibria between the ligand and polymer. Beyond the 1∶1 ratio, the subsequent addition of $Zn(ClO_4)_2$ caused new spectral changes (Figure 2(b)). The low-energy absorption at 387 nm was slightly blue-shifted to 376 nm after 4 equiv. of $Zn(ClO_4)_2$ was added in total, indicating that the coordination polymer partially decomposed when the metal-to-ligand ratio was above 1∶1. The titration with $Cd(ClO_4)_2$ gave almost the same result (see Figures 2(c) and 2(d)). Thus, it could be concluded that a metallo-supramolecular complex formed in solution when the metal-to-ligand ratio was 1∶1. In this type of linear polymer, each metal ion is coordinated with two ligands and the ditopic ligand is also coordinated with two metal ions through two perpy moieties. The changing trend in absorption at two characteristic wavelengths (287 and 387 nm) for two titration experiments is shown in Figure S15, revealing that the change of the predominant species involved in the self-assembly process at different metal-to-ligand ratios. In this solution, the three chromophores such as free ligand, 1∶1 metal-to-ligand, and 1∶2 metal-to-ligand complex exist in dynamic equilibrium so that the expected manner can be mediated by controlling the different ratios of ligand and metal ion. Like the traditional stepwise polymerization, the precise controlling of equal ratio of ligand and metal ion is a key to obtain the polymers with high molecular weight.

Emission spectra

It is well known that the photoluminescence (PL) behavior of compounds is highly dependent on the solvents, so the solution of ligand and polymers in different solvents was measured to test the solvatochromism effect. The PL properties in different solvents were examined by exciting the lowest-energy absorption maxima bond. It was found that the solvent polarity imposed strong influence on the wavelength and intensity of fluorescence emission (Figures 3, 4 and S16). For ligand **L**, the fluorescence peaks emerge around 430 nm in low polarity solvents like chloroform, dichloroethane, and THF. The peaks, however, exhibit a significant red-shift in polarity solvents (Table 2). The emission of **L** is largely quenched in solvents such as H_2O, methanol, and acetone due to the poor solubility. The fluorescence emissions of polymers show stronger dependence of solvent polarity than **L** and the light-emitting color and intensity differ significantly in different solvents. They show yellow light emission in solvents such as chloroform, dichloroethane, H_2O, and acetonitrile with emission peaks above 520 nm. However, the light-emitting shows apparent blue-shift in DMF and DMSO so that the emission colors changed to cyan-blue. Under the same concentration, the fluorescence intensity of **P1** in chloroform is the strongest but the emission is largely quenched in acetone, acetonitrile, and methanol. In aqueous media, the emission of **P1** is quenched but still visible clearly by naked eyes. As for **P2**, it shows the strongest emission in DMSO and also displays the relatively weak fluorescence emission in aqueous media. The PL spectra of the spin-coated thin films of **P1** and **P2** were investigated as well, they both exhibited luminescence emission similar to the situation in low polarity solvents (Figure S17).

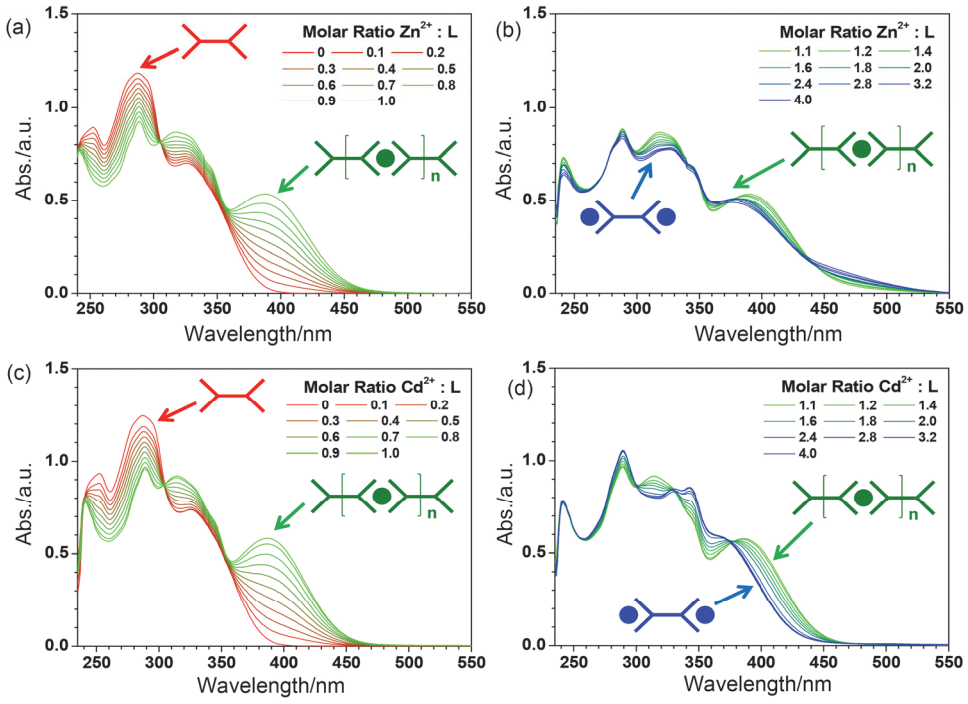

Figure 2 UV-vis spectra acquired upon titration of **L** in chloroform (4.0×10^{-5} mol/L) with $Zn(ClO_4)_2$ and $Cd(ClO_4)_2$, respectively. Shown are spectra at selected M^{2+}: L ratios ranging from 0 to 1 (a, c) and above 1 (b, d).

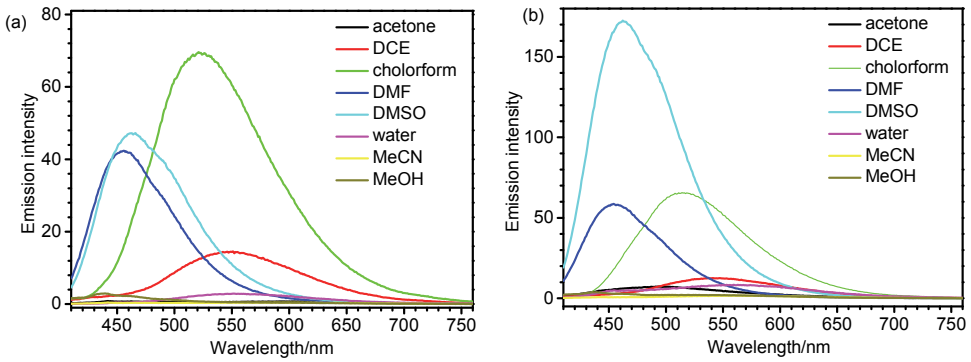

Figure 3 PL spectra of **P1** (a) and **P2** (b) in different solvents under the excitation at 390 nm (4.0×10^{-5} mol/L).

Table 2 Emission data of **L**, **P1**, and **P2** in different solvents and polymer films

Solvent	Solution						Film			
	λ_{max}[a]/nm			Stokes shift/cm^{-1}			λ_{max}[b]/nm		Stokes shift/cm^{-1}	
	L	**P1**	**P2**	**L**	**P1**	**P2**	**P1**	**P2**	**P1**	**P2**
Acetone	446	602	494	7699	10416	10152				
DCE	442	542	537	7956	12414	16343				
$CHCl_3$	426	521	514	7201	6713	6385				
DMF	452	456	454	12598	12913	12696	536	526	8444	7167
DMSO	460	462	463	12863	12957	13124				
H_2O	462	551	558	6524	16453	10650				
MeCN	450	591	557	8359	18045	16890				
MeOH	389	440	438	9258	12238	12134				

[a] 4.0×10^{-5} mol/L in different solvents; [b] Thin film on a quartz glass substrate.

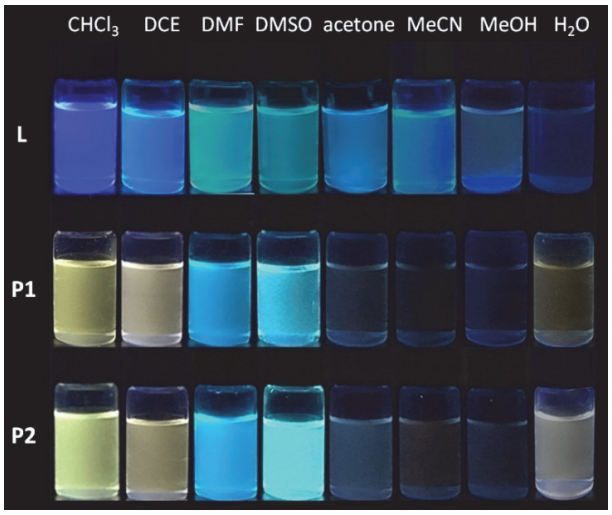

Figure 4 The emission colors of **L**, **P1**, and **P2** in different solvents (4.0×10^{-5} mol/L) under UV illumination at 365 nm.

Detection of nitroaromatic explosives

The visible emission of polymers in aqueous media prompted us to explore the possibility of their potential application as FCs for the detection of NACs. First, picric acid (PA) was selected as a model compound to test the fluorescence variation towards **P1** and **P2**. As expected, two polymers both displayed the sensing behavior towards PA. After the addition of PA to the aqueous solution of polymers, the fluorescence quenching caused an obvious color change that could be easily observed by naked eye. Two polymers both exhibited very high quenching efficiency. The fluorescence emission of **P1** and **P2** was quenched by 85% and 99% upon the addition of 1 equiv. of PA, resulting in the almost disappearance of the yellow light emission (Figures 5 and S18). The Stern-Volmer plot was used to study the response to PA of two polymers quantitatively (Figures 5(b) and S18(b)). Under low concentration, the Stern-Volmer constants were determined to be 5.08×10^5 mol^{-1}•L for **P1** and 1.77×10^6 mol^{-1}•L for **P2**, respectively.

Fluorescence quenching methods are dominant in fluorescence based explosives sensors.[23] Up to date, researchers have developed numerous mechanisms responsible for fluorescence quenching process that include photo-induced electron transfer (PET), resonance energy transfer (RET), electron exchange (EE), intermolecular charge transfer (ICT), inner filter effect (IFE), *etc*.[15,24] Because there is little spectral overlap between the emission of polymers and the absorption of PA, the RET approach is unfavorable (Figure S19). Electron and charge transfer processes, such as PET, ICT, and EE, are common approaches in fluorescence quenching. However, no new absorption peak but decreased absorption intensity could be observed with the increasing concentration of PA (Figure S20), so the possible mechanisms

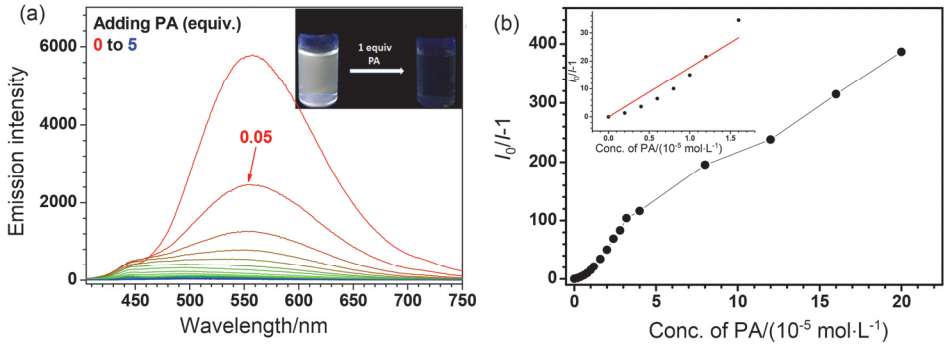

Figure 5 (a) Changes in fluorescence spectra of **P2** (4.0×10^{-5} mol•L^{-1}) with the addition of PA in water. Inset: change in the emission color after the addition of 1 equiv. of PA (under UV illumination at 365 nm); (b) Stern-Volmer plot in response to PA. Inset: Linear Stern-Volmer plot obtained at lower concentration range of PA.

such as PET, ICT, or EE can not be verified at this stage which need in-depth study by time-resolved transient spectrum in the future. Based on the strong IFE of PA over that of other NACs, the IFE should be considered as one of the major processes in the fluorescence quenching. The Stern-Volmer plots show non-linearity at higher concentration range, meaning the process is complicated which may be combined with diverse mechanisms.

Subsequently, in order to inspect the selectivity of these polymers towards PA, several other representative nitro-containing aromatic explosives (NACs), including 2-methyl-1,3,5-trinitrobenzene (TNT), 3,5-dinitrophenol (*m*-DNP), 4-nitrophenol (*p*-NP), 1-chloro-2,4-dinitrobenzene (CDNB), 2,6-dimethyl-4-nitrophenol (DMNP), 1,3-dinitrobenzene (DNB), 4-nitrobenzoic acid (NBA), and 4-nitrobenzaldehyde (NBD) were tested as well. Compared with PA, all other NACs displayed insignificant efficiency of the emission quenching (Figures S21 and S22). The fluorescence quenching efficiencies (η) upon adding 1 equiv. of different NACs towards **P1** and **P2** are presented in Figure 6. Although the fluorescence emission was almost totally quenched by PA, the quenching efficiencies for other NACs were relatively low and the same tendency was also observed in the measurement of K_{SV} constant (Table S1). Among these NACs, PA possesses the strongest acidity and lowest HOMO-LUMO gap, which may account for the high sensitivity and good selectivity. The good detection toward PA further demonstrates that IFE is one major process in the fluorescence quenching. The anti-interference ability of this type of polymers was investigated as well. It was found that, in the presence of 1 equiv. of other NACs, the fluorescence responses of **P2** to PA were unaffected in efficiency (Figure S23). These results further verified the high sensitivity and selectivity of this type coordination polymer for PA detection. The emerge of free ligand's emission peak indicates that the polymers may decompose when large amounts of NACs were added.

Finally, we explored the potential applications of this type of FCs so that the facile PA detection outdoors could be carried out. Test strips were prepared through dip-coating the acetonitrile solution of **P1** and **P2** into filter paper and then drying under vacuum. The test stripts both showed strong yellow light emission in the solid state. After dropping the test strips into PA dilute aqueous solution, no emission could be observed by naked eye under 365 nm UV light (Figure 7). So these type FCs based test strips display the potential facile applications in detecting the NACs pollution for the outdoor water.

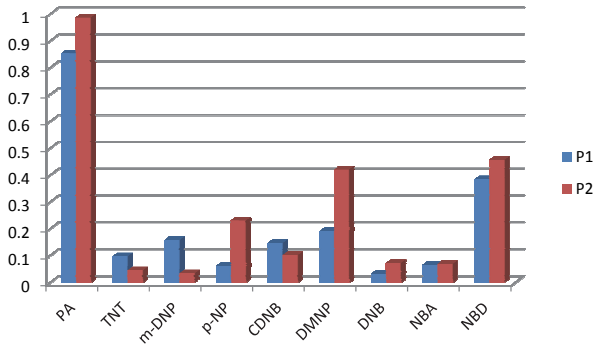

Figure 6 Fluorescence quenching efficiencies towards **P1** and **P2** (4.0×10^{-5} mol•L^{-1}) in water after the addition of 1 equiv. of various NACs.

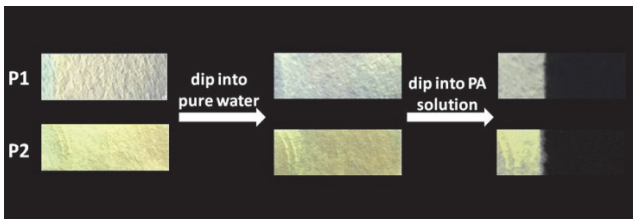

Figure 7 Images (under UV illumination at 365 nm) of **P1** and **P2** on test strips before and after diping into the pure water and PA diluted aqueous solution (1.0×10^{-5} mol•L^{-1}).

Conclusions

In summary, we synthesized one ditopic terpy-de-

rived conjugated ligand containing hydrophilic oligoethyoxy side chain via Suzuki coupling reaction. The ligand could coordinate with Zn^{2+} and Cd^{2+} ions to construct linear metallo-supramolecular coordination polylmers whose dispersibilities were significantly improved in organic solvent and water through the introduction of tetraethyleneglycol monomethyl ether side chain. Due to the large Stokes shift caused by the conjugated structure of the ligand and the inductive effect of the d^{10} transition metal ions, the polymers showed yellow light emission in chloroform and water and obvious blue-shift took place in polar solvents like DMF and DMSO. This type of coordination polymers displayed good selectivity and high sensitivity in the detection of PA in aqueous media. These visual FCs could be prepared into solution-coated test strips to achieve the facile detection outdoors, exhibiting the practical applications for public safety and security in the future.

Acknowledgement

This work is supported by the National Natural Science Foundation of China (Nos. 21371043 and 21302035), and the Fundamental Research Funds for the Central Universities (No. 2014HGCH0009). Y.-Y.Z. expresses the most sincere respect to Prof. Xi-Kui Jiang (Shanghai Institute of Organic Chemistry) and Prof. Zhan-Ting Li (Fudan University) for sustained encouragement and support for his research.

References

[1] Desvergne, J. P.; Czarnik, A. W. *Chemosensors of Ion and Molecule Recognition*, Kluwer Academic Publishers, Boston, **1997**.

[2] (a) Bhattacharjee, Y. *Science* **2008**, *320*, 1416; (b) Germain, M. E.; Knapp, M. J. *Chem. Soc. Rev.* **2009**, *38*, 2543; (c) Hu, Z.; Deibert, B. J.; Li, J. *Chem. Soc. Rev.* **2014**, *43*, 5815.

[3] Akhavan, J. *Chemistry of Explosives*, 2nd ed., Royal Society of Chemistry, London, **2004**.

[4] (a) Bingham, E.; Cohrssen, B.; Powell, C. H. *Patty's Toxicology*, John Wiley & Sons, New York, **2000**, IIB, p. 980; (b) Perez, G. V.; Perez, A. L. *J. Chem. Educ.* **2000**, *77*, 910.

[5] (a) Ashbrook, P. C.; Houts, T. A. *ACS Div. Chem. Health Safety* **2003**, *10*, 27; (b) Cameron, M. *Picric Acid Hazards*, American Industrial Hygiene Association, Fairfax, VA, **1995**.

[6] (a) Toal, S. J.; Trogler, W. C. *J. Am. Chem. Soc.* **2006**, *16*, 2871; (b) Salinas, Y.; Martinez-Manez, R.; Marcos, M. D.; Sancenon, F.; Costero, A. M.; Parra, M.; Gil, S. *Chem. Soc. Rev.* **2012**, *41*, 1261.

[7] (a) Swager, T. M. *Acc. Chem. Res.* **1998**, *31*, 201; (b) Hong, Y.; Lam, J. W. Y.; Tang, B. Z. *Chem. Commun.* **2009**, 4332; (c) Thomas, S. W.; Joly, G. D.; Swager, T. M. *Chem. Rev.* **2007**, *107*, 1339.

[8] (a) Yang, J.-S.; Swager, T. M. *J. Am. Chem. Soc.* **1998**, *120*, 5321; (b) Sohn, H.; Sailor, M. J.; Magde, D.; Trogler, W. C. *J. Am. Chem. Soc.* **2003**, *125*, 3821; (c) Rose, A.; Zhu, Z.; Madigan, C. F.; Swager, T. M.; Bulovic, V. *Nature* **2005**, *434*, 876; (d) Qu, Y.; Liu, Y.; Zhou, T.; Shi, G.; Jin, L. *Chin. J. Chem.* **2009**, *27*, 2043.

[9] (a) Braga, D.; Curzi, M.; Johansson, A.; Polito, M.; Rubini, K.; Grepioni, F. *Angew. Chem., Int. Ed.* **2006**, *45*, 142; (b) Lan, A.; Li, K.; Wu, H.; Olson, D. H.; Emge, T. J.; Ki, W.; Hong, M.; Li, J. *Angew. Chem., Int. Ed.* **2009**, *48*, 2334; (c) Nagarkar, S. S.; Joarder, B.; Chaudhari, A. K.; Mukherjee, S.; Ghosh, S. K. *Angew. Chem., Int. Ed.* **2013**, *52*, 2881; (d) Guo, Y.; Feng, X.; Han, T.; Wang, S.; Lin, Z.; Dong, Y.; Wang, B. *J. Am. Chem. Soc.* **2014**, *136*, 15485; (e) Ye, J.; Zhao, L.; Bogale, R. F.; Gao, Y.; Wang, X.; Qian, X.; Guo, S.; Zhao, J.; Ning, G. *Chem.-Eur. J.* **2015**, *21*, 2029; (f) Chen, M.-M.; Zhou, X.; Li, H.-X.; Yang, X.-X.; Lang, J.-P. *Cryst. Growth Des.* **2015**, *15*, 2753; (g) Yang, J.; Wang, Z.; Hu, K.; Li, Y.; Feng, J.; Shi, J.; Gu, J. *ACS Appl. Mater. Interfaces* **2015**, *7*, 11956; (h) Wang, B.; Lv, X.-L.; Feng, D.; Xie, L.-H.; Zhang, J.; Li, M.; Xie, Y.; Li, J.-R.; Zhou, H.-C. *J. Am. Chem. Soc.* **2016**, *138*, 6204; (i) Bogale, R. F.; Ye, J.; Sun, Y.; Sun, T.; Zhang, S.; Rauf, A.; Hang, C.; Tian, P.; Ning, G. *Dalton Trans.* **2016**, *45*, 11137.

[10] (a) Gole, B.; Shanmugaraju, S.; Bar, A. K.; Mukherjee, P. S. *Chem. Commun.* **2011**, *47*, 10046; (b) Zhang, Y.; Zhan, T.-G.; Zhou, T.-Y.; Qi, Q.-Y.; Xu, X.-N.; Zhao, X. *Chem. Commun.* **2016**, *52*, 7588.

[11] (a) Kumar, M.; Reja, S. I.; Bhalla, V. *Org. Lett.* **2012**, *14*, 6084; (b) He, X.; Zhang, P.; Lin, J.-B.; Huynh, H. V.; Muňoz, S. E. N.; Ling, C.-C.; Baumgartner, T. *Org. Lett.* **2013**, *15*, 5322; (c) Xiong, J.-F.; Li, J.-X.; Mo, G.-Z.; Huo, J.-P.; Liu, J.-Y.; Chen, X.-Y.; Wang, Z.-Y. *J. Org. Chem.* **2014**, *79*, 11619; (d) Yan, X.; Wang, H.; Hauke, C. E.; Cook, T. R.; Wang, M.; Lal Saha, M.; Zhou, Z.; Zhang, M.; Li, X.; Huang, F.; Stang, P. J. *J. Am. Chem. Soc.* **2015**, *137*, 15276.

[12] (a) Zhang, K.; Zhou, H.; Mei, Q.; Wang, S.; Guan, G.; Liu, R.; Zhang, J.; Zhang, Z. *J. Am. Chem. Soc.* **2011**, *133*, 8424; (b) Naddo, T.; Che, Y. K.; Zhang, W.; Balakrishnan, K.; Yang, X. M.; Yen, M.; Zhao, J.-C.; Moore, J. S.; Zang, L. *J. Am. Chem. Soc.* **2007**, *129*, 6978.

[13] (a) Dobrawa, R.; Lysetska, M.; Ballester, P.; Grune, M.; Würthner, F. *Macromolecules* **2005**, *38*, 1315; (b) Beck, J. B.; Ineman, M.; Rowan, S. J. *Macromolecules* **2005**, *38*, 5060; (c) Fustin, C. A.; Guillet, P.; Schubert, U. S.; Gohy, J. F. *Adv. Mater.* **2007**, *19*, 1665; (d) Kumpfer, J. R.; Rowan, S. J. *J. Am. Chem. Soc.* **2011**, *133*, 12866; (e) Wang, F.; Zhang, J.; Ding, X.; Dong, S.; Liu, M.; Zheng, B.; Li, S.; Wu, L.; Yu, Y.; Gibson, H. W.; Huang, F. *Angew. Chem., Int. Ed.* **2010**, *49*, 1090; (f) Chen, S.-G.; Yu, Y.; Zhao, X.; Ma, Y.; Jiang, X.-K.; Li, Z.-T. *J. Am. Chem. Soc.* **2011**, *133*, 11124; (g) Yan, X.; Xu, D.; Chi, X.; Chen, J.; Dong, S.; Ding, X.; Yu, Y.; Huang, F. *Adv. Mater.* **2012**, *24*, 362; (h) Tian, Y.-K.; Shi, Y.-G.; Yang, Z.-S.; Wang, F. *Angew. Chem., Int. Ed.* **2014**, *53*, 6090.

[14] (a) Dobrawa, R.; Würthner, F. *Chem. Commun.* **2002**, 1878; (b) Yu, S.-C.; Kwok, C.-C.; Chan, W.-K.; Che, C.-M. *Adv. Mater.* **2003**, *15*, 1643; (c) Chen, Y.-Y.; Tao, Y.-T.; Lin, H.-C. *Macromolecules* **2006**, *39*, 8559; (d) Popovic, Z.; Busby, M.; Huber, S.; Calzaferri, G.; De Cola, L. *Angew. Chem., Int. Ed.* **2007**, *46*, 8898; (e) Stepanenko, V.; Stocker, M.; Muller, P.; Buchner, M.; Würthner, F. *J. Mater. Chem.* **2009**, *19*, 6816; (f) Schlutter, F.; Wild, A.; Winter, A.; Hager, M. D.; Baumgaertel, A.; Friebe, C.; Schubert, U. S. *Macromolecules* **2010**, *43*, 2759; (g) Kokado, K.; Chujo, Y. *Dalton Trans.* **2011**, *40*, 1919; (h) Sato, T.; Higuchi, M. *Chem. Commun.* **2012**, *48*, 4947; (e) Sato, T.; Pandey, R. K.; Higuchi, M. *Dalton Trans.* **2013**, *42*, 16036; (f) Wu, Z.; Huang, X. *Chin. J. Chem.* **2016**, *34*, 703; (g) Liu, Z.; Lai, B.; Wen, H.; Robbins, J.; Huang, N. *Chin. J. Chem.* **2016**, *34*, 1304.

[15] Sun, X.; Wang, Y.; Lei, Y. *Chem. Soc. Rev.* **2015**, *44*, 8019.

[16] Li, H.-Q.; Ding, Z.-Y.; Pan, Y.; Liu, C.-H.; Zhu, Y.-Y. *Inorg. Chem. Front.* **2016**, *3*, 1363.

[17] (a) Han, F. S.; Higuchi, M.; Kurth, D. G. *Adv. Mater.* **2007**, *19*, 3928; (b) Han, F. S.; Higuchi, M.; Kurth, D. G. *J. Am. Chem. Soc.* **2008**, *130*, 2073.

[18] Hinderberger, D.; Schmelz, O.; Rehahn, M.; Jeschke, G. *Angew. Chem., Int. Ed.* **2004**, *43*, 4616.

[19] Liu, S.; Jin, Z.; Teo, Y. C.; Xia, Y. *J. Am. Chem. Soc.* **2014**, *136*, 17434.

[20] Wittmeyer, P.; Traser, S.; Sander, R.; Sondergeld, K. B.; Ungefug, A.; Weiss, R.; Rehahn, M. *Macromol. Chem. Phys.* **2016**, *217*, 1473.

[21] Wu, D.; Shao, T.; Men, J.; Chen, X.; Gao, G. *Dalton Trans.* **2014**, *43*, 1753.

[22] (a) Neese, F. *ORCA–An ab initio*, *Density Functional and Semiempirical Program Package*, version 3.0.3, Max-Planck Institute for Bioinorganic Chemistry, Mülheim an der Ruhr, Germany, **2015**; (b) Schafer, A.; Horn, H.; Ahlrichs, R. *J*. *Chem*. *Phys*. **1992**, *97*, 2571; (c) Schafer, A.; Huber, C.; Ahlrichs, R. *J*. *Chem*. *Phys*. **1994**, *100*, 5829.

[23] (a) McQuade, D. T.; Pullen, A. E.; Swager, T. M. *Chem*. *Rev*. **2000**, *100*, 2537; (b) Sohn, H.; Sailor, M. J.; Magde, D.; Trogler, W. C. *J*. *Am*. *Chem*. *Soc*. **2003**, *125*, 3821.

[24] Rong, M.; Lin, L.; Song, X.; Zhao, T.; Zhong, Y.; Yan, J.; Wang, Y.; Chen, X. *Anal*. *Chem*. **2015**, *87*, 1288.

(Zhao, X.)

